



ELSEVIER

Contents lists available at ScienceDirect

Developmental Biology

journal homepage: www.elsevier.com/locate/developmentalbiology

Foxp1/2/4 regulate endochondral ossification as a suppresser complex

Haixia Zhao^{a,1}, Wenrong Zhou^a, Zhengju Yao^a, Yong Wan^a, Jingjing Cao^a, Lingling Zhang^a, Jianzhi Zhao^a, Hanjun Li^a, Rujiang Zhou^a, Baojie Li^a, Gang Wei^b, Zhenlin Zhang^c, Catherine A. French^d, Joseph D. Dekker^e, Yingzi Yang^f, Simon E. Fisher^{g,h}, Haley O. Tucker^e, Xizhi Guo^{a,*}^a Bio-X Institutes, Key Laboratory for the Genetics of Developmental and Neuropsychiatric Disorders (Ministry of Education), Shanghai Jiao Tong University, Shanghai 200240, China^b Shanghai Institutes for Biological Sciences, Chinese Academy of Sciences (CAS), Shanghai 200032, China^c Department of Orthopedic Surgery, Shanghai Jiao Tong University Affiliated the Sixth People's Hospital, Shanghai, China^d Champalimaud Neuroscience Programme, Champalimaud Centre for the Unknown, Lisbon, Portugal^e Institute for Cellular and Molecular Biology, University of Texas at Austin, Austin, TX 78712, USA^f Developmental Genetics Section, National Human Genome Research Institute, NIH, MD 20892, USA^g Language and Genetics Department, Max Planck Institute for Psycholinguistics, Nijmegen, The Netherlands^h Donders Institute for Brain, Cognition and Behaviour, Radboud University, Nijmegen, The Netherlands

ARTICLE INFO

Article history:

Received 22 September 2014

Received in revised form

3 December 2014

Accepted 4 December 2014

Available online 17 December 2014

Keywords:

Foxp1

Foxp2

Foxp4

Endochondral ossification

Osteoblast

Transcriptional repressor

ABSTRACT

Osteoblast induction and differentiation in developing long bones is dynamically controlled by the opposing action of transcriptional activators and repressors. In contrast to the long list of activators that have been discovered over past decades, the network of repressors is not well-defined. Here we identify the expression of Foxp1/2/4 proteins, comprised of Forkhead-box (Fox) transcription factors of the Foxp subfamily, in both perichondrial skeletal progenitors and proliferating chondrocytes during endochondral ossification. Mice carrying loss-of-function and gain-of-function *Foxp* mutations had gross defects in appendicular skeleton formation. At the cellular level, over-expression of *Foxp1/2/4* in chondrocytes abrogated osteoblast formation and chondrocyte hypertrophy. Conversely, single or compound deficiency of *Foxp1/2/4* in skeletal progenitors or chondrocytes resulted in premature osteoblast differentiation in the perichondrium, coupled with impaired proliferation, survival, and hypertrophy of chondrocytes in the growth plate. Foxp1/2/4 and Runx2 proteins interacted *in vitro* and *in vivo*, and Foxp1/2/4 repressed Runx2 transactivation function in heterologous cells. This study establishes Foxp1/2/4 proteins as coordinators of osteogenesis and chondrocyte hypertrophy in developing long bones and suggests that a novel transcriptional repressor network involving Foxp1/2/4 may regulate Runx2 during endochondral ossification.

© 2014 Elsevier Inc. All rights reserved.

Introduction

The axial and appendicular skeletons form through a process of endochondral ossification. During this process, mesenchymal progenitor cells within the cartilage anlage differentiate to chondrocytes. The chondrocytes then mature through resting, proliferating, and hypertrophic stages, and are finally replaced by invading osteoblasts and blood vessels (Kronenberg, 2003). Meanwhile, skeletal progenitor cells within the perichondrium are progressively committed to an osteoblast lineage (Karsenty and Wagner,

2002; Long and Ornitz, 2013). The perichondrium is the major reservoir of osteoblast precursors in developing long bones (Maes et al., 2010), and osteoblast differentiation in the perichondrium is tightly regulated by the progressive action of osteoblast-specific transcription factors (Hartmann, 2009; Karsenty, 2008; Kobayashi and Kronenberg, 2005; Kronenberg, 2003; Long, 2012).

An array of cofactors, such as Maf, Taz, Satb2, Gli2, Dlx5, Bapx1 and Msx2, promotes osteoblast differentiation by stimulating Runx2 expression or enhancing Runx2 activity (Long, 2012). Runx2 is an early transcription factor that integrates multiple osteogenic signals to induce mesenchymal progenitor cells toward osteogenic commitment (Ducy et al., 1997; Komori et al., 1997; Otto et al., 1997). During endochondral bone formation, some of these osteogenic signals come from chondrocytes. For instance, *Ihh* secreted by prehypertrophic and hypertrophic chondrocytes promotes osteoblast differentiation by activating Runx2. After Runx2 stimulates osteogenic

* Corresponding author. Fax: +86 021 34206736.

E-mail address: xzguo2005@sjtu.edu.cn (X. Guo).¹ Development and Regeneration Key Lab of Sichuan Province, Department of Anatomy and Histology and Embryology, Chengdu Medical College, Chengdu, Sichuan Province, 610500, China.

commitment, Osterix and ATF4 sequentially enforce the differentiation and maturation of these osteoblasts (Ducy et al., 1996; Nakashima et al., 2002; Yang et al., 2004). Conversely, osteoblast differentiation is suppressed by repressors such as Twist1, Hand2, Zfp521, Schn3, Stat1, Tle, Hey, Hes and Hdac4, which perturb DNA binding or nuclear translocation by Runx2, decrease Runx2 protein expression, or degrade Runx2 protein (Javed et al., 2010; Long, 2012). Loss of Runx2 activators or cofactors impairs bone formation or homeostasis (Komori et al., 1997), and genetic inactivation of Runx2 repressors leads to enhanced osteoblast differentiation or ectopic ossification. For instance, *Hand2* null mice displayed enhanced ossification in the branchial arch (Funato et al., 2009).

The Fox family of transcription factors, characterized by a highly conserved forkhead DNA-binding domains, are essential for regulating several developmental processes (Augello et al., 2011; Eijkelenboom and Burgering, 2013; Katoh et al., 2013; Kume, 2011; Raychaudhuri and Park, 2011). For example, the *Foxp1/2/3/4* subfamily regulates differentiation or proliferation of cardiomyocytes (Wang et al., 2004; Zhang et al., 2010), B and T cells (Duhon et al., 2012; Feng et al., 2009; Hu et al., 2006; Wang et al., 2014), ES cells (Gabut et al., 2011) and various malignant cell-types (Chen et al., 2011; Koon et al., 2007; Korac et al., 2009). This subfamily regulates cell differentiation through transcriptional repressor activity. *Foxp1/2/4* proteins generally show overlapping expression patterns in the lung, gut, and brain during development (Lu et al., 2002; Shu et al., 2007; Takahashi et al., 2008), and in some cases, these proteins are known to act cooperatively (Li et al., 2012, 2004). However, the role of *Foxp1/2/4* genes in bone development remains unclear. In this report, we employ genetic, histological and molecular approaches to investigate the role of *Foxp* genes during endochondral ossification. Our findings identify the *Foxp1/2/4* complex as a novel Runx2 suppressor that regulates endochondral ossification.

Materials and methods

Mice

The *Foxp1^{fl/fl}* (Feng et al., 2009), *Foxp2^{fl/fl}* (French et al., 2007), transgenic mice *Prx1-Cre* (Logan et al., 2002) and *Col2-Cre* mice (Lu et al., 2013) have been described in previous studies. For transgenic mice generation, *Foxp1* (NM_053202.2) cDNA, *Foxp2* (BC058960) cDNA and *Foxp4* (BC057110) cDNA were individually driven by *Col2a1* promoter and enhancer as previously reported (Yang et al., 2003). The genotyping primers for the *Col2-Foxp1*, *Col2-Foxp2*, *Col2-Foxp4* and *Foxp4^{fl/fl}* mice are provided in [Supplementary material Table S1](#). The genetic backgrounds of all knockout mice were uniform mixtures of 129S1/SvIMJ and C57Bl/6J. All transgenic mice were ICR background. All animal procedures were performed in accordance with protocols set by Shanghai Jiao Tong University (SYXK 2011-0112).

Generation of *Foxp4* conditional knockout mice

Two *Loxp* sites were inserted into the *Foxp4* gene at introns 9 and 14 ([Supplementary material Fig. S4A](#)). The targeted ES clones were identified by PCR using primers P1/P2 and P3/P4 that generate 5473 bp and 4648 bp products, respectively ([Supplementary material Fig. S4B](#)). The conditional allele of *Foxp4^{fl}* is genotyped by primers P5/P6 as a 290 bp fragment. *Foxp4* was efficiently deleted by Cre activity, as evidenced by the decreased levels of *Foxp4* mRNA and protein in the E13.5 limbs from *Prx1-Cre; Foxp4^{fl/fl}* mice ([Supplementary material Fig. S4D](#) and [E](#)). Mice of homozygous *Foxp4^{fl/fl}* showed no obvious abnormality throughout life, suggesting the *Foxp4^{fl}* allele functions normally.

Skeletal preparation, histological, IHC analyses and lacZ staining

Paraffin and frozen sections of skeletal samples from the transgenic and knockout mice at E15.5, E16.5 and E18.5 were obtained and processed as previously reported (Guo et al., 2004). Sections were stained as previously described using H&E for general histology (Beyotime), von Kossa for analysis of mineralization, and safranin O for analysis of proteoglycans (Guo et al., 2004). The primary antibodies for IHC were the following: anti-Osterix (1:50, Abcam, ab22552), anti-Runx2 (1:50, Santa Cruze, sc-10758), anti-Collagen Type I (1:50, Millipore, AB765P), anti-Foxp1 (1:50, Millipore, ABE68), anti-Foxp2 (1:200, Abcam, ab16046), anti-Foxp4 (1:50, Millipore, ABE74), anti-Patched (1:50, Santa Cruze, sc-6149), anti-Ihh (1:50, Santa Cruze, sc-1196), anti-Flag (1:100, Agilent Technologies, 200472), anti-His (1:100, GenScript, A00174), and anti-BrdU (1:100, Abcam, ab6326). The secondary antibodies used were the Alexa Fluor 488 conjugated (1:200, Invitrogen, A-21206) and the Alexa Fluor 594 conjugated second antibody (1:200, Invitrogen, A-11058 or A-11032). Mounting was performed with DAPI fluorescent dye (Southern Biotech). Fluorescent microscopic images were taken using a Leica SP5 confocal microscope. For LacZ staining, the samples were at first performed by whole mount X-gal staining as done previously (Day et al., 2005), and then re-fixed and sectioned with 10 μ m thick to observe the Cre enzyme activity.

In situ hybridization BrdU labeling and TUNEL assay

In situ hybridization for whole mount embryos or sections was performed using digoxin-labeled probes as previously described (Guo et al., 2009). Fragments of *Foxp1* (NM_053202.2) cDNA, *Foxp2* (BC058960) cDNA and *Foxp4* (BC057110) cDNA were amplified by PCR and subcloned into the pGEM-T vector to generate RNA probes, respectively. All the oligos are provided in [Supplementary material Table S1](#). Other probes have been described previously: *Sox9*, *Col2a1*, *Col10a1*, *Mmp13*, *Opn*, *Ihh*, *Pthrp*, *Osx*, *Col1a1* (Akiyama et al., 2004; Guo et al., 2004). For bromodeoxyuridine (BrdU) labeling, mice received an intraperitoneal injection of BrdU (100 μ g/g of body mass; Sigma). Two hours later, mice were sacrificed and embedded in paraffin for sectioning. TUNEL staining was performed using Dead-End™ Fluorometric TUNEL System kit (Promega) according to the manufacturer's instructions.

Luciferase reporter assay, cell culture and qRT-PCR

HEK-293T or Cos7 cells with a density of 0.5×10^5 were plated in 24-well tissue and cultured until 90% confluent. Cells were transfected according to manufacturer's instructions using lipo-fectamine™ 2000 (Invitrogen). Expression plasmids for p6OSE2-luc, pOG2-luc, pOG2mOSE2-luc reporter constructs have been described previously (Ducy and Karsenty, 1995). Cos7 cells were transfected with p6OSE2-luc (0.08 μ g) or pOG2mOSE2-luc (0.08 μ g) reporter plasmid together with the following expression plasmids as indicated: Flag-Runx2 (0.24 μ g), His-Foxp1, His-Foxp2, His-Foxp4, His-Foxp1-N (0.48 μ g), His-Foxp1-M (0.48 μ g), His-Foxp1-N-M (0.48 μ g) and His-Foxp1-C (0.48 μ g). *Foxp1/2/4* dose-dependent transcriptional repression of Runx2 was assayed using *Foxp*: Runx2 ratios of 1:3, 1:1, 2:1. HEK-293T cells were transfected with p6OSE2-luc (0.16 μ g) reporter plasmid together with the following expression plasmids as indicated: Flag-Runx2 (0.16 μ g), Flag-Runx2-Runt (0.16 μ g), His-Foxp1 (0.16 μ g), His-Foxp2 (0.16 μ g) and His-Foxp4 (0.16 μ g). 4 ng pCMV-Renilla-luciferase plasmid (Promega) was used for normalization. Empty pCDNA3.0 vector DNA was used to equalize the total amount of DNA for all transfection assays. Luciferase assays were performed 48 h after transfection by using the Dual Luciferase Kit (Promega).

The full-length cDNA of *Foxp4* (BC057110) or *EGFP* (used as control) was amplified by PCR and subcloned into the PMSCVpuro retroviral vector. Retrovirus was generated by transfection of PMSCVpuro-*Foxp4* construct or PMSCVpuro-*GFP* construct into Platinum-E Retroviral packaging cells using FuGENE 6 (Roche). ATDC5 cells were cultured in a medium of DMED/F-12 supplemented with 5% FBS (Invitrogen). To induce chondrogenic differentiation of ATDC5 cells, the cells upon reaching confluence were induced by differentiation medium by addition of insulin (10 µg/ml, Sigma), human transferrin (10 µg/ml, Sigma), and sodium selenite (10 µg/ml, Sigma). The ATDC5 cells overexpressing *Foxp4* or *GFP* protein were obtained by retroviral infection and puromycin resistance selection. Similar overexpression was performed in MC3T3 cells. MC3T3 cells were cultured in α -MEM medium (Invitrogen) including 10% FBS. For osteogenic introduction, the cells were cultured in the medium with addition of 10 mM β -glycerolphosphate (Sigma), 50 µg/ml ascorbic acid (Sigma), and 10 nM dexamethasone (Sigma). Alcian blue staining for ATDC5 cells was performed as previously report (Atsumi et al., 1990). For Alizarin Red S staining, MC3T3 cells were fixed in 10% formalin for 30 min and stained by 40 mM Alizarin Red S solution (pH 4.2) (Sigma).

RNA was extracted from cultured cells using the Trizol reagent (Invitrogen) according to standard procedures. SuperScriptTM III First-Strand Synthesis System (Invitrogen) was used to reverse-transcribe RNA. Real-time PCR was performed on ABI Prism 7500 Sequence Detection System (Applied Biosystems) using a FastStart universal SYBR Green Master (ROX) kit (Roche). The samples were normalized to actin expression. All primer sequences for *Foxp4* quantification could be found in [Supplementary material Table S1](#).

Plasmids

The epitope-tagged derivatives of full-length *Foxp1* (NM_053202.2), *Foxp2* (BC058960), *Foxp4* (BC057110) or *Runx2* (NM_001146038), containing carboxy-terminal His, carboxy-terminal Myc or amino-terminal Flag tags as indicated were cloned in the pcDNA3.0 vector (Invitrogen). The constructs encoding different domains of *Runx2* (NT, Runt, Runx1, NT-Runt or Runt-Runx1) or *Foxp1* (N, M(LZ/ZF), C(FH), N-M(LZ/ZF)) as schematically drawn in [Figs. 7 and 8](#) were amplified by PCR, and products with amino-terminal Flag tags or carboxy-terminal His tags respectively were inserted into the pcDNA3.0 vector.

Co-IP/IP assay

Co-IP assays were performed by transfecting HEK-293T cells with the indicated plasmids using lipofectamineTM 2000 (Invitrogen). After 48 h, cells were harvested. Cell extracts were subjected to immunoprecipitation with either the anti-Myc antibody (1/2000, Roche, 11667149001), anti-His (1/2000, GenScript, A00174) or anti-Flag (1/2000, Agilent Technologies, 200472) antibody as indicated for overnight at 4 °C. The antibody was coupled to protein A/G PLUS-Agrose (Santa Cruze, sc-2003). The immunoprecipitates were washed eight times with washing buffer and analyzed by SDS-PAGE and immunoblotting with antibody as indicated. For *in vivo* analysis, Nuclear extracts from E13.5 limb were immunoprecipitated with anti-Foxp1 antibody (Millipore, ABE68), anti-Foxp2 antibody (Abcam, ab16046) or IgG (Santa Cruze, sc-2027), and then blotted with anti-Foxp1 (1/1000, Millipore, ABE68), anti-Foxp2 (1/2000, Abcam, ab16046), anti-Foxp4 antibody (1/1000, Millipore, ABE74) and anti-Runx2 antibody (1/1000, Santa Cruze, sc-10758) as indicated.

Statistical analyses

Statistical analysis was performed by Student's *t* test using GraphPad Prism 5 software. Data are represented as mean \pm SEM, and significance was set at $p \leq 0.05$. For BrdU labeling, at least three individual samples analyzed and five to ten consecutive sections from each sample were taken into account.

Results

Foxp1/2/4 genes are expressed in developing long bones

Expression patterns of the *Foxp1/2/4* genes were examined in the limb skeletons during endochondral ossification by *in situ* hybridization and immunohistochemistry (IHC). At the E12.5 stage of early skeletal primordial formation, *in situ* hybridization showed redundant expression of *Foxp1/2/4* in the digit ray of forelimbs as well as hindlimbs, partially overlapping with expression of *Sox9* and *Gdf5* in the perichondrium and joint ([Figs. 1A and S1A](#)). Similarly, *in situ* hybridization showed redundant expression of *Foxp1/2/4* in the perichondrium/periosteum of E13.5 digits and E16.5 humerus ([Fig. 1A and B](#)). In IHC analysis of consecutive sections of E16.5 distal humerus, the range of *Foxp1/2/4* expression in the perichondrium was similar to *Runx2*, but differed from that of the osteoblast marker *Osx* (arrows in [Fig. 1C, a–e](#)), implying that *Foxp1/2/4* may be active in the same cell types as *Runx2*. Indeed, the *Foxp1/2/4* proteins were mostly located in the nuclei of perichondrial cells, partially overlapping with the *Runx2* distribution (arrows in [Fig. S1B](#)). In addition to the expression of *Foxp1/2/4* in perichondrium, *Foxp2* and *Foxp4* were detected at relatively lower levels in proliferating chondrocytes ([Fig. 1C, b and c](#)). These results demonstrate that the murine *Foxp1/2/4* genes are redundantly expressed in the perichondrium and proliferating chondrocytes of developing long bones.

Over-expression of *Foxp1/2/4* in chondrocytes abrogates skeletal ossification

To investigate the roles of *Foxp1/2/4* in skeletogenesis, we generated transgenic mice that overexpress *Foxp1*, *Foxp2*, and *Foxp4* transgenic mice in chondrocytes under the control of *Col2a1* promoter and enhancer. We obtained two or three independent founders for each transgene. The severity of the ossification defect varied between founders with the same transgene, possibly due to the variances in copy number or ectopic expression levels of the transgene. The founders with the most severe defects were selected for further study. The over-expression of *Foxp1/2/4* in the chondrocytes of skeletons from each transgenic mouse was validated by IHC with anti-Foxp1, anti-Foxp2 or anti-Foxp4 polyclonal antibodies ([Fig. S2](#)). The *Col2-Foxp1*, *Col2-Foxp2* and *Col2-Foxp4* transgenic mice all showed perinatal lethality and smaller size compared to wild-type controls ([Fig. 2A](#)). The transgenes produced remarkable defects in endochondral ossification, as indicated by decreased Alizarin red staining in skeletal preparations of forelimbs and hindlimbs of transgenic mice compared to controls ([Fig. 2A, b–b'' and c–c''](#)). In contrast to the development of long bones, Alizarin red staining in the skulls was impaired in a relatively less extent in the transgenic embryos ([Fig. 2A, d–d''](#)). Therefore, overexpression of *Foxp1/2/4* in chondrocytes inhibits endochondral ossification.

The expression of *Col2a1* was relatively decreased in the chondrocytes from *Foxp* transgenic skeletons ([Fig. 2B, b–b''](#)). In addition, marked decreases of *Col10a1* (hypertrophic chondrocyte marker, B, c–c'' and Bg, Bg', B, i–i''), *Opn* (osteoblast marker, [Fig. 2B, e–e'' and k–k''](#)) and *Col1a1* (osteoblast marker, [Fig. 2B, f–f'' and](#)

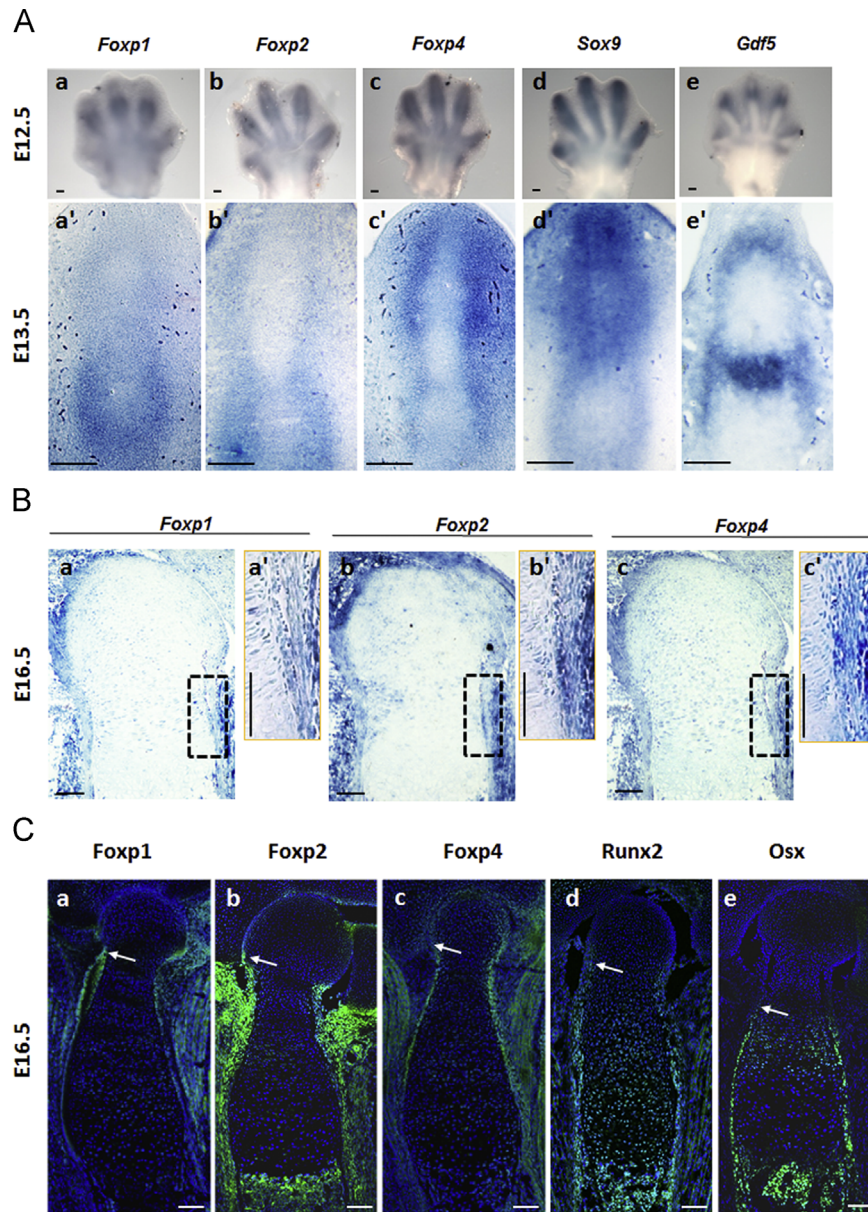


Fig. 1. Expression of *Foxp1/2/4* in the limb during skeletal development. (A) Detection of *Foxp1/2/4* expression by *in situ* hybridization in skeletal primordium at E12.5 (A, a–c) and E13.5 (A, a'–c'). Expression of *Foxp1/2/4* is mainly observed in surrounding perichondrium. Expression of *Sox9* and *Gdf5* is also shown in (Ad–e) and (Ad'–e'). (B) Detection of *Foxp1/2/4* expression in serial sections of the proximal tibia at E16.5. (Ba'), (Bb') and (Bc') show the enlargement of the boxed regions in (Ba), (Bb) and (Bc), respectively. (C) IHC for *Foxp1/2/4*, *Runx2* and *Osterix* (*Osx*) in serial sections of E16.5 distal humerus, counterstained with DAPI (blue). Arrows designate the onset of expression of *Foxp*, *Runx2* and *Osx*, respectively, in the E16.5 proximal humerus. Scale bar: 100 μ m.

l–l'), safranin O (Fig. 2B, a–a'') and von Kossa (Fig. 2B, d–d'') staining showed greatly reduced chondrocyte hypertrophy and osteoblast differentiation in the growth plates of transgenic embryos relative to wild-type controls. Consistent with these findings, the expression of *Ihh* and *Ptch1* was significantly abrogated in the *Col2-Foxp2* transgenic embryos (Fig. S2D). Notably, the *Col2-Foxp1* and *Col2-Foxp4* transgenic embryo appeared to retain small mineralized domains in scapula whereas the *Col2-Foxp2* mice had no mineralization at all (Fig. 2A, b'–b'').

To validate the suppressive role of *Foxp* genes in chondrocyte hypertrophy and osteoblast differentiation, ATDC5 cells that are capable of undergoing a chondrogenesis *in vitro* under induction were transfected by *Foxp4*-expressing retrovirus. Compared to GFP-expressing control retrovirus, the *Foxp4*-overexpressing cells showed remarkably reduced mRNA expression of *Col10a1*, *Runx2* by 14 days post-transfection as well as lower levels of *Ptch1* and *Gli1* expression

by 21 days post-transfection (Fig. S3A–C). It displayed diminished Alcian blue staining 21 days post-transfection (Fig. S3D). These results are consistent with our *in vivo* results. In addition, over-expression of *Foxp4* in MC3T3 osteoblast precursor cells repressed osteogenic differentiation, as evaluated by Alizarin red staining at 21 days post-transfection (Fig. S3E). Collectively, these findings suggest that over-expression of *Foxp1/2/4* in chondrocytes severely impairs chondrocyte hypertrophy and osteoblast differentiation.

Foxp deficiency in perichondrium and chondrocytes perturbs skeletal development

To further assess the role of *Foxp1/2/4* in cartilage and bone development, we used *Col2-Cre* to generate mice lacking *Foxp* in the perichondrium and chondrocytes. Confirming that the *Col2-Cre* mice we used have Cre activity in the perichondrium and

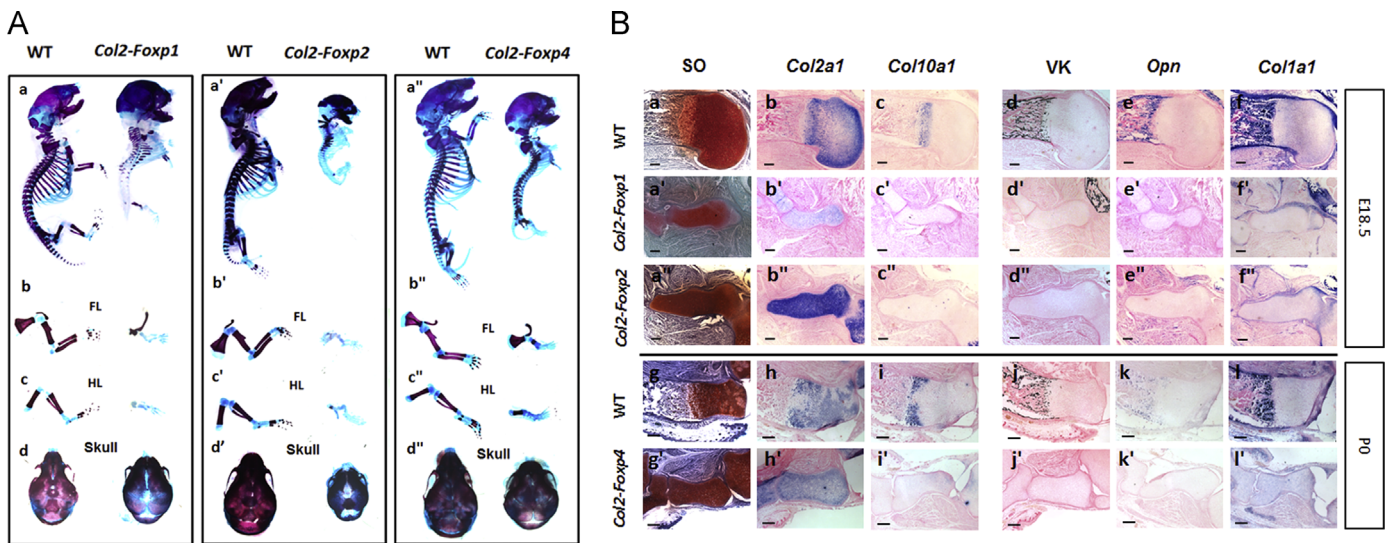


Fig. 2. Abrogated chondrocyte hypertrophy and endochondral ossification in the *Foxp1/2/4* transgenic mice. (A) Skeletal preparations from wild-type and *Col2-Foxp1/2/4* transgenic mice. Bone is stained by Alizarin red, whereas cartilage is stained by Alcian blue. Skeletons of the *Col2-Foxp1* (Aa–d) and *Col2-Foxp2* (Aa'–d') mice were examined at E18.5, whereas skeletons of the *Col2-Foxp4* (Aa''–d'') mice were analyzed at P0. Lateral views of whole skeletons are shown in (Aa), (Aa') and (Aa''); forelimbs are shown in (Ab), (Ab') and (Ab''); hindlimbs are shown in (Ac), (Ac') and (Ac''); dorsal view of skulls are shown in (Ad), (Ad') and (Ad''). (B) Indicated markers of bone development were detected by *in situ* hybridization in serial sections of the E18.5 humeri from the *Col2-Foxp1/2* transgenic mice and in the P0 tibia from the *Col2-Foxp4* transgenic mice. Safranin O staining and von Kossa staining are also shown in (Ba, Ba', Ba'', Bg, Bg') and (Bd, Bd', Bd'', Bj, Bj'). The *Col10a1*-positive structure in Fig. 2Bc'' should be the scapula. The van Kossa positive structure in 2Bd'' is the clavicle. Scale bar: 200 μ m.

chondrocytes, LacZ staining was evident in the perichondrium and chondrocytes of *Col2-Cre; R26R* reporter mice (Fig. S5A). The *Foxp1/2/4* genes were targeted individually or in combination, and IHC or western blot showed near-complete elimination of *Foxp* expression in the intended tissue (Figs. S4D, E and S5B). However, growth of heterozygous mice *Col2-Cre; Foxp4^{fl/fl}* was significantly arrested at 2 weeks of age, precluding the generation of homozygous *Col2-Cre; Foxp4^{fl/fl}* mutant mice. Therefore, *Col2-Cre; Foxp4^{fl/+}* mice were used to assess the role of *Foxp4* in long bone development. Not surprisingly, the phenotype of single knockout mice was less severe than the phenotype of the compound knockout mice. The single knockout mice survived postnatally for a long period up to 1 year. In contrast, *Foxp1/2* and *Foxp1/4* compound knockout mice (*Col2-Cre; Foxp1/2^{fl/fl}* and *Col2-Cre; Foxp1^{fl/fl}; Foxp4^{fl/+}*) died perinatally, possibly due to the severe skeletal dysgenesis described below.

To analyze skeletal deformities in *Foxp* mutant mice at E18.5 and P10, overall skeletal preparations were analyzed with Alcian blue and Alizarin red staining. At E18.5, the overall body size and the appendicular skeleton were shortened in the single and compound *Foxp* mutants compared to the wild-type controls (Fig. 3A). By P10, the severity of attenuated skeletal growth increased as the genetic dosage of *Foxp1/2* decreased (Fig. 3C). Defective skeletal development was not limited to the appendicular skeletons, as bone malformations were also detected in the skull. In the *Col2-Cre; Foxp1/2^{fl/fl}* and *Col2-Cre; Foxp1^{fl/fl}; Foxp4^{fl/+}* compound mutants, both the cranium and nasal defects included shortened nasal bones (double head arrows) and disruption of basisphenoid bone development (yellow arrows) of the cranial base in the compound mutants (Fig. 3B, a–f). Together, these observations suggest that *Foxp* genes cooperatively regulate skeletal development in a dose-dependent manner.

To identify the molecular changes associated with defective skeletal development in the *Foxp* mutants, we performed histological and IHC analyses in sections from E18.5 tibia of mutant and control mice (Fig. 4). In the control tibia sections, von Kossa staining showed initiation of mineralization in the perichondrium/periosteum cells neighboring hypertrophic chondrocytes (outlined in Fig. 4A, A'). In contrast, in the compound *Foxp* mutant mice, we observed precocious mineralization extending to perichondrial cells neighboring the proliferating chondrocytes (marked by

arrows in Fig. 4D, D' and E, E'). This effect was observed, but much more subtle in the single mutant.

In agreement with these results, osteoblast differentiation in the perichondrium was advanced in the compound mutant mice compared to the control, as indicated by the elevated expression of osteoblast markers *Osx* (Figs. 4I, J and 5A, g–h), *Coll* (Figs. 4N, O, 5 Ak–l) and *Opn* (Fig. 4S and T). These findings demonstrate advanced osteoblast differentiation, maturation and mineralization during endochondral ossification in *Foxp*-deficient mice. Therefore, we hypothesized that the *Foxp* genes may regulate osteogenic commitment.

Foxp deficiency in skeletal progenitor cells leads to precocious osteogenic commitment

To explore the effect of *Foxp* deficiency on osteogenic commitment of skeletal progenitor cells, we used *Prx1-Cre* to eliminate *Foxp* in the mesenchymal progenitor cells (Logan et al., 2002). Like the *Col2-Cre* knockout mice, which lack *Foxp* in the perichondrium and chondrocytes, the *Prx1-Cre; Foxp1/2^{fl/fl}* compound knockout mice had osteogenic defects. Compound knockout of *Foxp* alleles with either *Prx1-Cre* or *Col2-Cre* resulted in relatively advanced expression of *Runx2* and *Osx* in the perichondrium of E15.5 humerus sections (arrows in Fig. 5A, a–h and a'–h'), suggesting that *Foxp* deficiency stimulates early osteogenic induction and commitment. Moreover, *Coll* expression was elevated in the perichondrium adjacent to proliferating chondrocytes osteoblast maturation in the compound *Foxp* mutant, indicative of advanced osteoblast maturation (arrows in Fig. 5A, i–l and i'–l'). These results suggest that *Foxp* deficiency in the mesenchymal progenitor cells leads to a premature osteogenic commitment.

Next we tested whether *Foxp* deficiency affected osteoblast proliferation in addition to osteogenic commitment. To assess osteoblast proliferation *in vivo*, E15.5 animals were treated with BrdU, and two hours later, BrdU was quantified in the proximal humerus. IHC analyses showed that a greater percentage of osteoblast defined by *Osx*-expressing cells, were BrdU positive in the *Prx1-Cre; Foxp1/2^{fl/fl}* mutants as compared to the *Foxp1/2^{fl/fl}* controls (Fig. 5Bm', Bn' and C). In addition, the *Osx*-expressing cell layers were expanded in the perichondrium of compound mutant

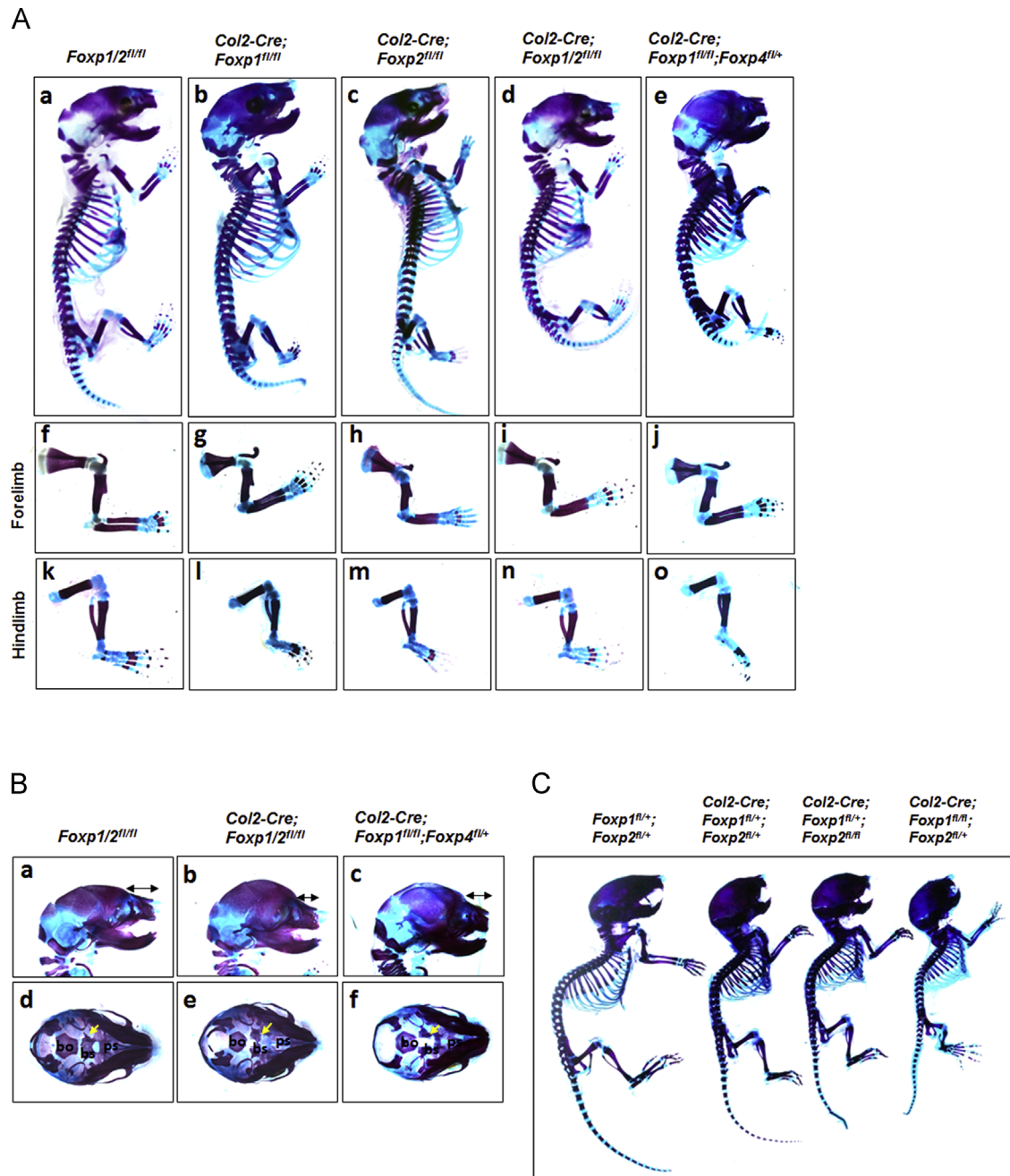


Fig. 3. Compound deficiency of *Foxp1/2/4* impairs skeletal growth. (A) Alizarin red/Alcian blue staining of skeletons isolated from the E18.5 *Col2-Cre; Foxp1^{fl/fl}*, *Col2-Cre; Foxp2^{fl/fl}*, *Col2-Cre; Foxp1^{fl/fl}; Foxp4^{fl/+}* embryos, including the whole skeleton (Aa–e), forelimb (Af–j), hindlimb (Ak–o). (B) Magnified view of E18.5 heads (Ba–f) in the *Col2-Cre; Foxp1^{fl/fl}* and *Col2-Cre; Foxp1^{fl/fl}; Foxp4^{fl/+}* mice, showing craniofacial malformations and shortening of the nasal bones. The formation of the cranial base bones (Bd–f, yellow arrows) is impaired in the mutants with respect to the controls. Bs, basisphenoid; bo, basioccipital; ps, presphenoid. (C) Skeletal preparations of the P10 *Col2-Cre; Foxp1^{fl/+}*, *Col2-Cre; Foxp1^{fl/+}; Foxp2^{fl/+}*, *Col2-Cre; Foxp1^{fl/+}; Foxp2^{fl/fl}*, *Col2-Cre; Foxp1^{fl/fl}; Foxp2^{fl/+}* mice (littermates). Bone is stained with Alizarin red, where as cartilage is stained with Alcian blue.

mice compared to controls (brackets in Fig. 5Bm', Bn' and C). These results suggest that *Foxp* deficiency in mesenchymal progenitor cells led to enhanced osteoblast proliferation. Collectively, these results support the hypothesis that *Foxp* genes are important for regulating osteogenic commitment, osteoblast proliferation and differentiation during endochondral ossification.

Foxp deficiency in the perichondrium and chondrocytes impairs chondrogenesis

In addition to regulating osteogenic commitment and development, the *Foxp* genes could affect skeletal development by

regulating chondrogenesis. To investigate this possibility, we performed histological analyses and *in situ* hybridization on E18.5 sections from the *Col2-Cre; Foxp* mutants and controls. Safranin O staining (brackets in Fig. 6A'–E') and *Col10a1* expression (brackets in Fig. 6F–J) were used to detect collagen II and hypertrophic chondrocytes, respectively, these analyses showed smaller domains of hypertrophic chondrocytes in the growth plates of E18.5 tibia from the single and compound mutant mice compared to controls. Confirming these results, the tibia of E15.5 mutants showed a shorter distance between the two *Col10a1*-expressing domains and shorter *Opn*- and *Mmp13*-expressing domains (double head arrows in Fig. S7A), indicative of decreased chondrocyte

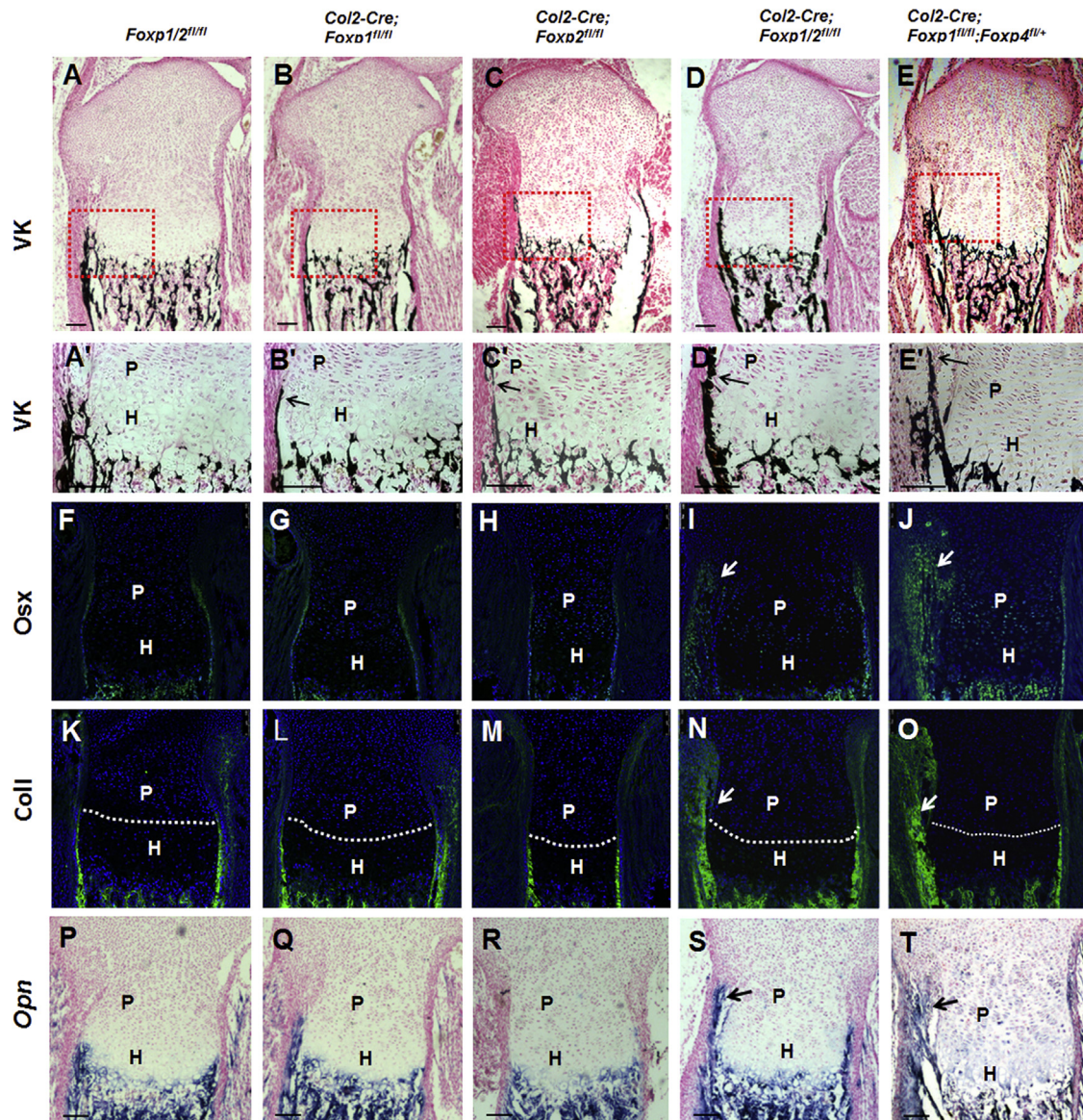


Fig. 4. Deletion of *Foxp1/2/4* by *Col2-Cre* advanced mineralization and osteoblast differentiation in the perichondrium. (A–E) Von Kossa staining of the equivalent sections of E18.5 tibiae (A–E); boxed regions are magnified in (A'–E'). (F–T) Expression of osteoblast markers *Osx* (F–J) and *Coll* (K–O) were detected by IHC, and *Opn* (P–T) was examined by *in situ* hybridization. The dashed lines delineate the proliferative/hypertrophic zone. P, proliferative zone; H, hypertrophic zone. Scale bar: 100 μ m.

hypertrophy. In contrast, the *Col2-Cre; Foxp1/2^{fl/fl}* mutant showed an increase in proliferating or prehypertrophic chondrocytes compared to the control, assessed by expression of *Ihh* and *Pthc1* (arrows in Fig. S7B). Therefore, *Foxp* deficiency may delay chondrocyte hypertrophy and maturation during endochondral ossification.

Next, to assess whether decreased proliferation or increased apoptosis might contribute to the reduction in hypertrophic chondrocytes, we performed the BrdU assay described above and TUNEL analysis in the proximal tibia of E18.5 mutants and the *Col2-Cre* control. Compared to the control, BrdU levels were significantly reduced in proliferating zones of all *Foxp* single and compound mutants and in the resting zones of all mutants except the *Foxp1* single mutant (Fig. 6K–O, U and V). TUNEL analysis showed significantly increased chondrocyte apoptosis in all the *Foxp* mutant mice except the *Foxp1* single mutant (Fig. 6P–T, W). Together, these data indicate that depletion of *Foxp* genes affects chondrocyte proliferation, survival and hypertrophy.

Foxp1/2/4 proteins inhibit the transcriptional activity of *Runx2*

The defects in endochondral ossification observed in *Foxp* deficient mice were opposite to previously described in *Runx2^{-/-}* mice (Komori et al., 1997; Takarada et al., 2013). Given the overlapping expression patterns of *Foxp* and *Runx2*, we suspected that *Foxp1/2/4* may influence osteogenic differentiation and chondrocyte hypertrophy by regulating *Runx2*. To address this possibility, we first examined the impact of *Foxp* proteins on *Runx2* transactivation *via* reporter assays employing luciferase constructs (pOG2-Luc or p6OSE2-Luc) driven by consensus *Runx2* binding sites in their promoters (Ducy and Karsenty, 1995). COS7 cells were transfected with the p6OSE2-Luc reporter and with *Runx2* and *Foxp* expression vectors as indicated. As expected, co-transfection of p6OSE2-Luc and the *Runx2* expression vector induced luciferase activity. Co-transfection of p6OSE2-Luc with *Runx2* and *Foxp1*, *Foxp2* or *Foxp4* significantly suppressed luciferase activity, with the extent of suppression dependent on the dose of *Foxp1*, *Foxp2*

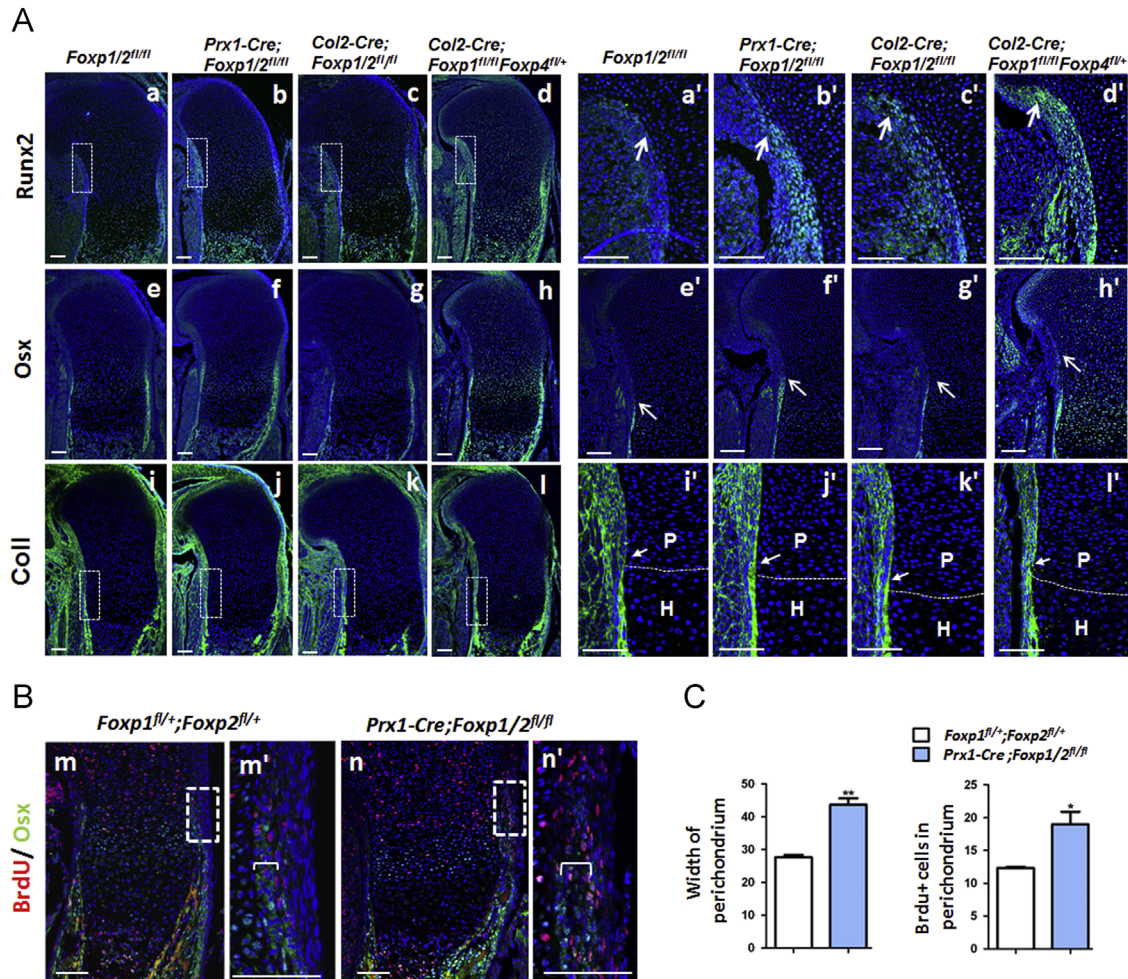


Fig. 5. Loss of *Foxp1/2/4* leads to precocious osteogenic commitment from mesenchymal progenitor cells. (A) IHC analysis of Runx2, Osx and Coll expression in equivalent sections of E15.5 humeri from the *Foxp1/2^{fl/fl}* (Aa, Ae, Ai), *Prx1-Cre; Foxp1/2^{fl/fl}* (Ab, Af, Aj), *Col2-Cre; Foxp1/2^{fl/fl}* (Ac, Ag, Ak) and *Col2-Cre; Foxp1^{fl/fl}; Foxp4^{fl/+}* (Ad, Ah, Al) embryos. The boxed regions in (Aa–d, i–l) are enlarged in (Aa'–d', i'–l'). Dashed lines delineate the proliferative/hypertrophic zone. (B) Double staining of BrdU (red) and Osx (green) in the equivalent sections of E15.5 humeri from *Foxp1^{fl/+}; Foxp2^{fl/+}* (Bm) and *Prx1-Cre; Foxp1/2^{fl/fl}* (Bn) embryos, counterstained with DAPI (blue). (Bm') and (Bn') are high-magnification images of the boxed regions in (Bm) and (Bn), respectively. (C) Quantitative analysis indicates that the width of Osx-positive domains and the percentage of BrdU+ cells over perichondrial DAPI-positive cells are increased in the mutant ($n=3$). Brackets indicate the width of Osx expression regions in the perichondrium. P, proliferative zone; H, hypertrophic zone. Scale bar: 100 μ m.

or Foxp4 (Fig. 7A). Interestingly, co-expressing various combinations of Foxp1/2/4 did not further suppress Runx2 transactivation activity beyond the suppression caused by single Foxp proteins at the same total dose (Fig. 7B). To confirm that Foxp proteins specifically suppressed Runx2-induced luciferase activity, we repeated the assay using the pOG2mOSE2-Luc reporter, in which the Runx2 binding sites are mutated. As expected, neither Runx2 nor the Foxp proteins significantly changed the luciferase activity of this construct. These results demonstrate that Foxp proteins can suppress Runx2 transactivation activity, suggesting that Foxp complexes may function as a negative regulator of Runx2 in osteoblast lineages.

Runt is the DNA binding domain of Runx2 protein and the Runt domain alone induced luciferase activity at levels comparable to full-length Runx2 protein. Interestingly, various Foxp proteins suppressed luciferase induction by the Runt domain (Fig. 7D), suggesting that these proteins may directly bind the Runt domain of Runx2. Foxp proteins contain forkhead, leucine-zipper and zinc-finger domains, which are responsible for DNA-binding and homotypic or heterotypic interactions, respectively (Wang et al., 2003). To determine which domain(s) are involved in Runx2 suppression, we created construct for expressing the Foxp1 N-terminal domain, middle domain (M, containing the leucine zipper and zinc finger

domain), or C-terminal domain (containing the forkhead domain) independently or the N-terminal and middle domains together. In the luciferase assay with full-length Runx2, each domain of Foxp1 suppressed Runx2 transactivation (Fig. 7E), although no single domain suppressed Runx2 activity as effectively as the full-length protein. Collectively, these findings suggest that Foxp complexes may downregulate Runx2 activity during endochondral ossification by interacting with the Runt domain.

The Foxp1/2/4 complex interacts with Runx2

To directly test whether Foxp1/2/4 proteins can interact with Runx2, we performed co-immunoprecipitation experiments on extracts from 293T cells cotransfected with Flag-tagged Runx2 and His- or Myc-tagged Foxp constructs. As shown in Fig. 8A–C, Runx2 protein was efficiently co-immunoprecipitated with each Foxp protein. In addition, IHC with anti-Flag and anti-His antibodies showed colocalization of Flag-tagged Runx2 and His-tagged Foxp1, 2, or 4 in the nuclei of cotransfected Cos7 cells (Fig. S8). Consistent with these *in vitro* results, endogenous Foxp1 was efficiently co-immunoprecipitated with Foxp2, Foxp4 and Runx2 in nuclear extracts from E13.5 limbs (Fig. 8D and E). These analyses

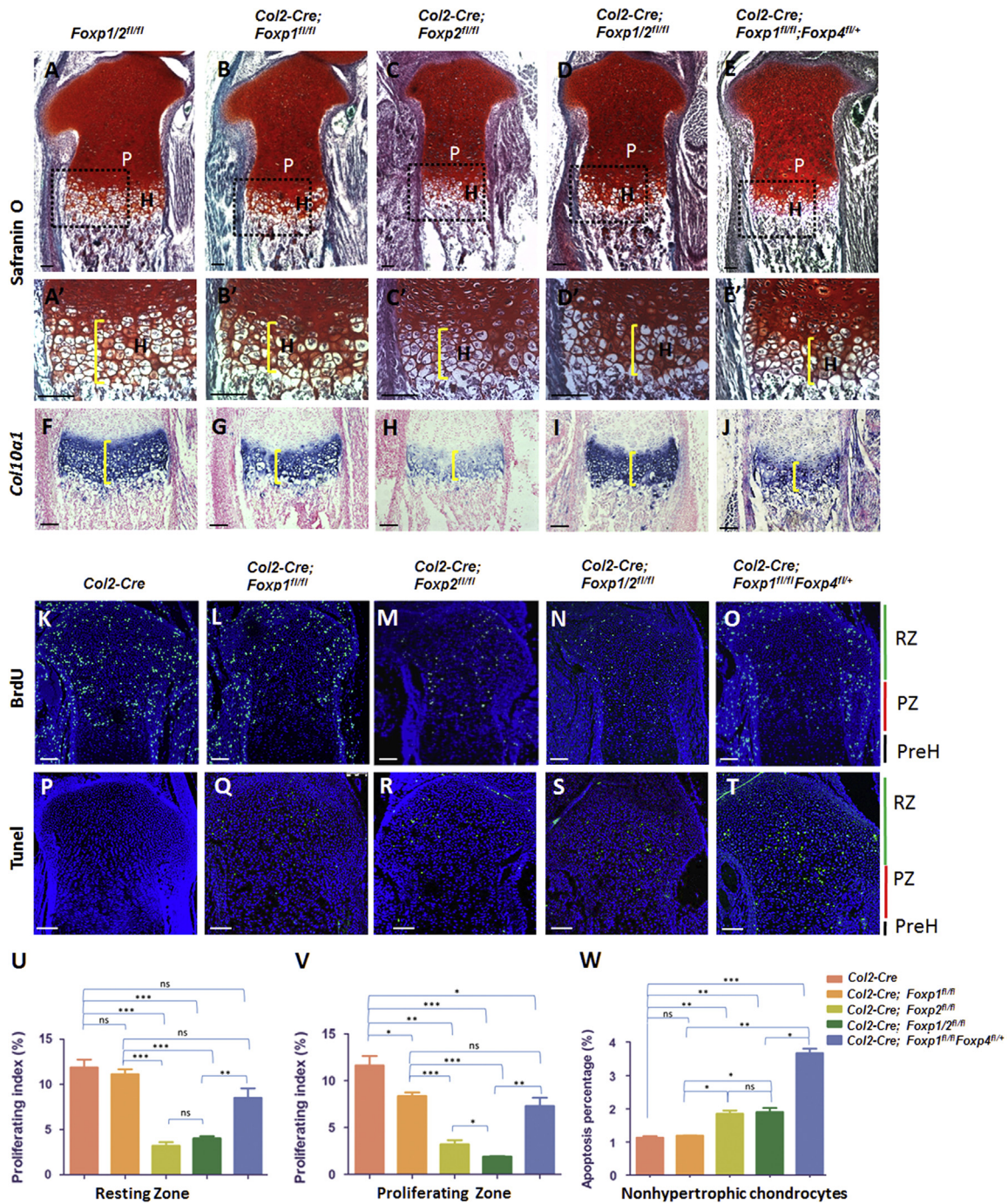


Fig. 6. Ablation of *Foxp1/2/4* impairs chondrocyte hypertrophy. (A–E) Safranin O staining of equivalent sections in E18.5 tibiae isolated from the various *Col2-Cre; Foxp* mutant mice. P, proliferative zone; H, hypertrophic zone. (A'–E') Magnification of the boxed region in (A–E). (F–J) Detection of *Col10a1* expression by *in situ* hybridization validates the shortened hypertrophic domains of the mutant tibiae. (K–O) IHC for BrdU in the sections from E18.5 proximal tibiae as detected by anti-BrdU staining. RZ: the resting zone; PZ: proliferating zone; PreH: prehypertrophic zone. (P–T) Apoptosis as detected by TUNEL assay in the sections from E18.5 proximal tibiae. RZ, PZ, PreH. (U–V) The proliferating indexes which mean the rate of BrdU-positive chondrocytes in all resting or proliferating chondrocytes in (K–O) were shown in (U) and (V), respectively. (W) Apoptosis percentage showing the rate of TUNEL-positive cells in all nonhypertrophic chondrocytes in (P–T). $n \geq 3$. ns: nonsense, (*) $p < 0.05$, (**) $p < 0.01$, (***) $p < 0.001$. Scale bar: 100 μ m.

demonstrate that *Foxp1/2/4* proteins interact with *Runx2* *in vivo* and *in vitro*.

To identify the domains involved in the interaction between *Foxp1/2* and *Runx2*, truncated forms of *Runx2* were cotransfected into Cos7 cells with Flag-tagged *Runx2*, and interactions were assessed by co-immunoprecipitation and His-tagged *Foxp1/2/4* vectors (Fig. 8G). All forms of *Runx2* that included the Runt domain interacted with *Foxp2*, while forms of *Runx2* that lacked the Runt

domain did not interact with *Foxp2* (Fig. S9). Next, we used co-immunoprecipitation to test whether the *Foxp1* C-terminal domain, which contains the forkhead domain, was sufficient for interactions with full-length *Runx2*. Indeed, the *Foxp1* C-terminal domain was co-immunoprecipitated with *Runx2* (Fig. 8F). Taken together, these results imply that *Foxp1/2/4* bind to *Runx2* via interactions between the *Runx2* Runt domain and the C-terminal domain of *Foxp* proteins.

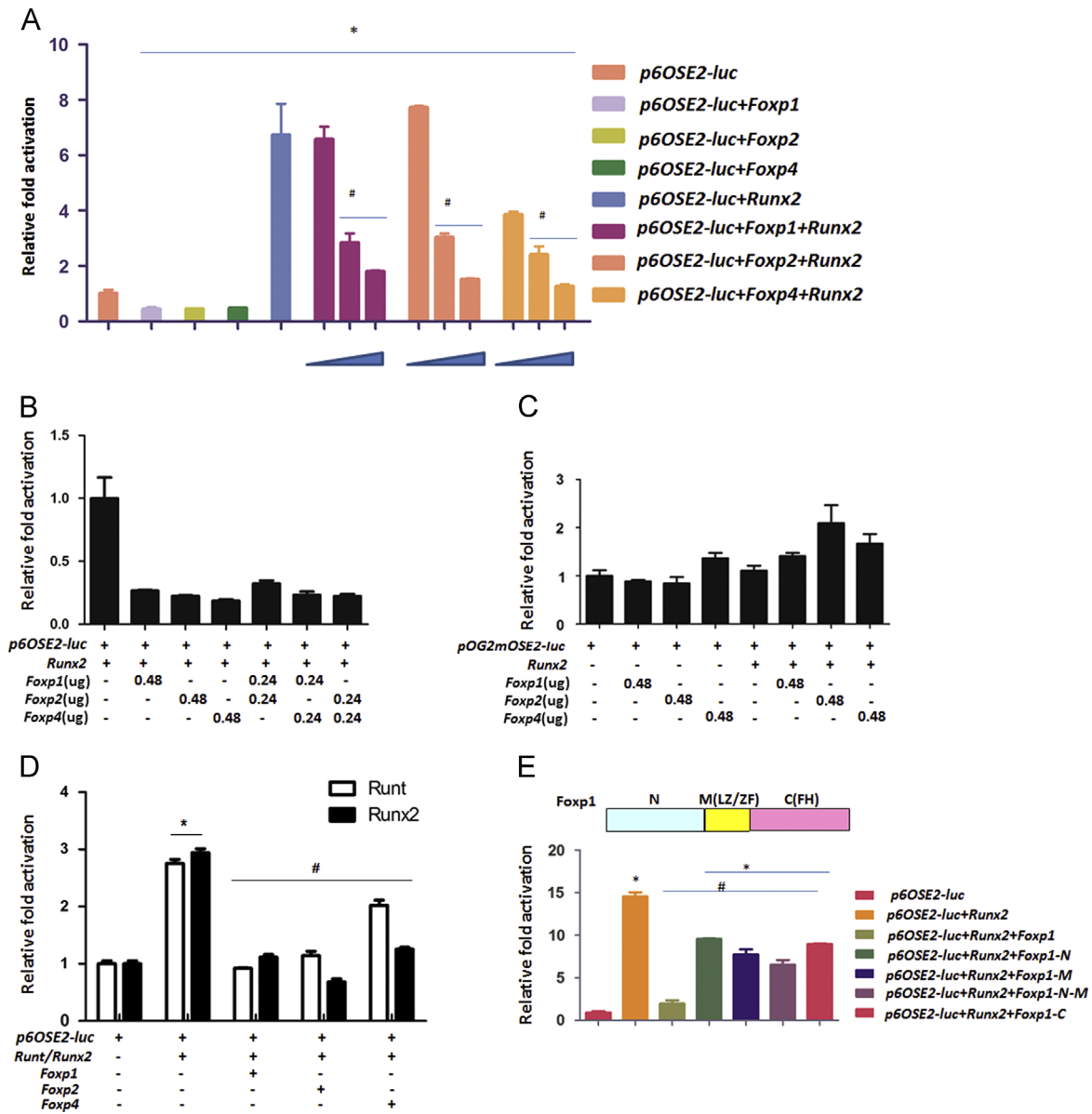


Fig. 7. Foxp1/2/4 inhibits the transcriptional activity of Runx2. (A) Transactivation by Runx2 was measured using a luciferase assay in Cos7 cells cotransfected with p6OSE2-Luc reporter (0.08 μg), Runx2 (0.24 μg) and increasing doses of Foxp1/2/4 expression constructs (at Foxp/Runx2 ratios: 1:3; 1:1; 2:1). (B) The effects of varying combinations of Foxp1/2/4 on Runx2-induced transactivation were assessed using a luciferase assay with the pOG2-Luc reporter in Cos7 cells, as described in A. (C) As a control, the luciferase assay was repeated in Cos7 cells using the pOG2mOSE2-Luc reporter, in which the Runx2 binding site required for Runx2 transactivation is mutated. (D) Transient cotransfection of the p6OSE2-Luc reporter with expression vectors for Runt domain, Runx2 and Foxp1/2/4 in HEK-293T cells. (E) Top panel: regions of Foxp1. N, N-terminus containing the poly(Q) region; M, middle, including the leucine zipper/zinc finger (LZ/ZF); and C, the C-terminal portion of Foxp1 employed for the transfections. Bottom panel: full-length or truncated forms of Foxp1 were transiently expressed in COS7 cells co-transfected with the p6OSE2-Luc reporter and Runx2, and Runx2-induced transactivation was analyzed as above. Data are shown as mean ± SEM, and n=3. Significance was determined by t-test. (*) P < 0.05, Foxp samples versus control. (#) P < 0.05, Foxp samples versus Runx2 or Runt.

Discussion

In this study, we investigated the role of Foxp genes during endochondral ossification by generating transgenic mice with gain-of-function and loss-of-function Foxp mutations. Overexpression of individual Foxp1/2/4 genes disrupted osteoblast differentiation and chondrocyte hypertrophy, while single or combined deficiency of Foxp1/2/4 led to precocious ossification and defective chondrogenesis in the growth plates. Thus, the Foxp1/2/4 proteins are important for proper long bone development. Substantiating this conclusion, we found that Foxp1/2/4 expression in the perichondrium and proliferating chondrocytes of appendicular skeletons overlaps with expression of Runx2, a central regulator of endochondral ossification. Moreover, Foxp1/2/4 physically interacts

with Runx2 and inhibits the transactivation function of Runx2. Collectively, these results implicate a novel pathway for the regulation of endochondral ossification.

We propose that Foxp1/2/4 proteins coordinate osteogenesis and chondrogenesis during long bone development by regulating Runx2 (Fig. 8K). This is a central factor in regulating bone development, as several repressors or corepressors, including Twist1/2, Zfp521 and Hdac4, have been reported to modulate osteoblast differentiation and chondrocyte hypertrophy through their differential interaction with Runx2 protein (Bialek et al., 2004; Correa et al., 2010; Hesse et al., 2010; Shimizu et al., 2010; Vega et al., 2004). Runx2 regulates osteoblast differentiation and chondrocyte hypertrophy partially through the induction of Ihh expression (Yoshida et al., 2004), and we detected altered Ihh

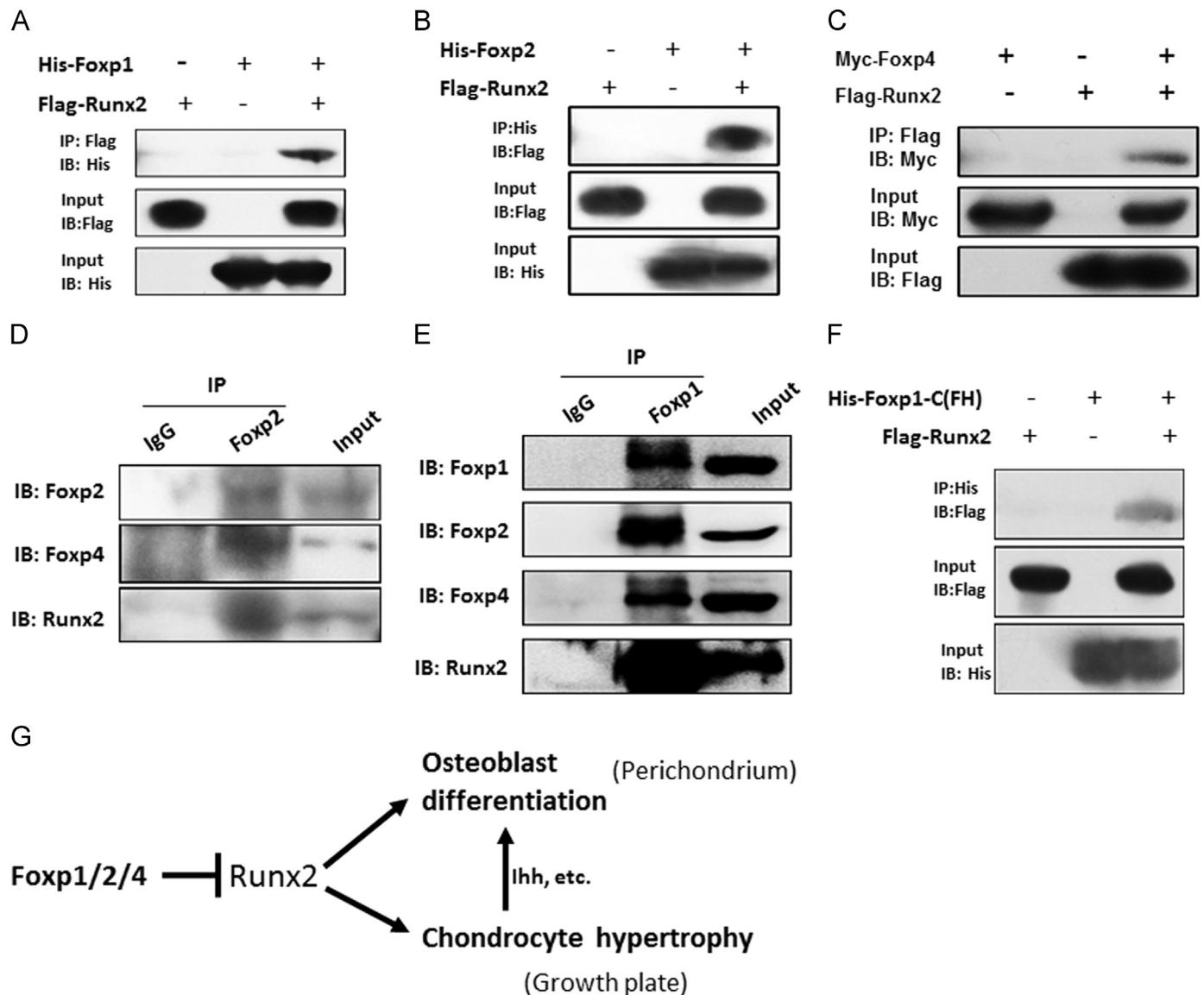


Fig. 8. Foxp1/2/4 physically interacts with Runx2. (A–C) *In vitro* interactions between Foxp1/2/4 and Runx2 were assessed by co-immunoprecipitation in HEK-293T cells cotransfected with the indicated vector combinations of His-Foxp1/Flag-Runx2 (A), His-Foxp2/Flag-Runx2 (B) or Myc-Foxp4/Flag-Runx2 (C). Cell lysates were prepared and co-immunoprecipitated with anti-Flag or anti-His and then blotted with anti-His, anti-Flag or anti-Myc. (D, E) To assess *in vivo* interactions of endogenous Foxp and Runx2, nuclear extracts prepared from E13.5 limbs were immunoprecipitated with anti-Foxp2 or IgG and blotted with anti-Foxp2, anti-Foxp4 or anti-Runx2 antibody (D), or immunoprecipitated with anti-Foxp1 antibody and blotted with anti-Foxp1, anti-Foxp2, anti-Foxp4 or anti-Runx2 antibody (E). (F) Runx2 co-immunoprecipitates with the C-terminal of Foxp1 containing forkhead (FH) domain (Foxp1-C). 293T cells were cotransfected with Flag-tagged Runx2 and the His-tagged Foxp1-C fragment, which included the forkhead domain (FH). Co-immunoprecipitation was performed as indicated. (G) Proposed mechanism by which the Foxp complex regulates osteogenesis and chondrocyte hypertrophy of the growth plate: Foxp1/2/4 complex regulates osteoblast differentiation and chondrocyte hypertrophy partially through inhibiting Runx2 activity.

signaling in the *Foxp* gain-of-function and loss-of-function mutants. Thus, dysregulated Runx2-induced *Ihh* signaling may account for the impaired osteoblast differentiation and chondrocyte hypertrophy in *Foxp* mutant mice.

Interestingly, *Foxp* deficiency in skeletal progenitor cells was associated with changes in Runx2 expression and cellular morphology in proliferating chondrocytes. Some proliferating chondrocytes in the *Foxp* mutants appeared to retain characteristics of prehypertrophic chondrocytes, with somewhat larger size and less organized arrangement compared to controls. In addition, expression of Runx2 and *Osx* was slightly elevated in perichondrium adjacent to resting or proliferating chondrocytes. Given that elevated Runx2 expression in the perichondrium has been shown to inhibit chondrocyte proliferation and hypertrophy (Hinoi et al., 2006), the gross defects in bone development in the *Foxp* mutants

may result from combined regulation of Runx2 activity in the perichondrium and proliferating chondrocytes. However, it is important to note that the Foxp proteins may coordinate osteogenesis and chondrogenesis *via* multiple pathways, including pathways that are independent of Runx2. For example, Foxo proteins have been reported to regulate osteoblast proliferation and differentiation through interactions with Runx2, CREB and ATF4 (Almeida, 2011; Kode et al., 2012).

Furthermore, although our data support shared roles for Foxp1/2/4 proteins in regulating endochondral ossification *via* Runx2, there are important differences in the expression patterns and contributions of individual Foxp1/2/4 proteins during bone development. These differences suggest that the individual Foxp1/2/4 proteins play overlapping yet distinct roles in regulating osteogenic targets. For example, the overlapping expression patterns of

Foxp1/2/4, *Sox9* and *Gdf5* in early digit rays indicated that *Foxp* genes are induced early in perichondrial skeletal progenitor cells. However, *Foxp4* was preferentially expressed in the distal digit at E12.5 and E13.5, while *Foxp1* expression was relatively enriched in the perichondrium of the second phalange. *Foxp2* showed moderate expression in the perichondrium of all digits. In terms of function, deletion of a single allele of *Foxp4* by *Col2-Cre* severely arrested skeletal growth and led to osteogenic defects as severe as those caused by the dual, homozygous deletion of *Foxp2* and *Foxp1*. Yet in some cases, deletion of *Foxp2* and/or *Foxp1* had a greater effect than deletion of *Foxp4*; for example, the ectopic activation of *lhh* signaling in resting/proliferating chondrocytes was more remarkable in the *Col2-Cre; Foxp1/2^{fl/fl}* mutant than in the *Col2-Cre; Foxp1^{fl/fl}; Foxp4^{fl/+}* mutant (Fig. S7B). In addition, *Foxp2* deficiency caused the most severe defects in chondrocyte proliferation while *Foxp1/4* deficiency had the greatest impact on chondrocyte apoptosis. Thus, although the *Foxp1/2/4* proteins have significant redundancy and may regulate common sets of target genes as a trimeric complex, it is likely that they also play differential roles in the regulation of osteoblast differentiation and chondrogenesis, perhaps through various combinations of homo- or hetero-dimers.

If distinct *Foxp* complexes have different roles in osteoblast differentiation and chondrogenesis, it follows that the *Foxp* genes should have context- and time-dependent functions in bone development. Indeed, while osteogenic differentiation was advanced in the long bones of the E15.5 *Prx1-Cre; Foxp1/2^{fl/fl}* mutant, ossification was retarded in the parietal skull bone (Fig. S6). Thus, *Foxp* proteins appear to context-dependent roles in endochondral and intramembranous ossification. Thus, *Foxp* proteins appear to play a complex series of regulatory roles in bone development, and these roles may vary with different protein complexes, developmental stages, and tissue contexts. Additional studies will be required to fully delineate these regulatory mechanisms. In conclusion, our study suggests that *Foxp1/2/4* proteins regulate endochondral ossification through their interaction with *Runx2* and suppression of *Runx2* activity. The study of *Foxp1/2/4* provides a new transcriptional repressor that differentially controls osteoblast differentiation and chondrocyte hypertrophy during long bone development.

Funding

This work was supported by grants to Xizhi Guo (the 973 program of China 2014CB942902 and 2012CB966903; NSFC 31171396, 31271553, 81421061 and 31100624), to Dr. Simon E. Fisher (UK Wellcome Trust, 080971) and to Dr. Haley Tucker (NIH/USA, R01CA31534).

Appendix A. Supporting information

Supplementary data associated with this article can be found in the online version at <http://dx.doi.org/10.1016/j.ydbio.2014.12.007>.

References

- Akiyama, H., Lyons, J.P., Mori-Akiyama, Y., Yang, X., Zhang, R., Zhang, Z., Deng, J.M., Taketo, M.M., Nakamura, T., Behringer, R.R., McCreary, P.D., de Crombrughe, B., 2004. Interactions between *Sox9* and *beta*-catenin control chondrocyte differentiation. *Genes Dev.* 18, 1072–1087.
- Almeida, M., 2011. Unraveling the role of *FoxOs* in bone—insights from mouse models. *Bone* 49, 319–327.
- Atsumi, T., Miwa, Y., Kimata, K., Ikawa, Y., 1990. A chondrogenic cell line derived from a differentiating culture of AT805 teratocarcinoma cells. *Cell Differ. Dev.* 30, 109–116.
- Angelino, M.A., Hickey, T.E., Knudsen, K.E., 2011. FOXA1: master of steroid receptor function in cancer. *EMBO J.* 30, 3885–3894.
- Bialek, P., Kern, B., Yang, X., Schrock, M., Sosic, D., Hong, N., Wu, H., Yu, K., Ornitz, D.M., Olson, E.N., Justice, M.J., Karsenty, G., 2004. A twist code determines the onset of osteoblast differentiation. *Dev. Cell* 6, 423–435.
- Chen, Z., Xiao, Y., Zhang, J., Li, J., Liu, Y., Zhao, Y., Ma, C., Luo, J., Qiu, Y., Huang, G., Korteweg, C., Gu, J., 2011. Transcription factors E2A, FOXO1 and FOXP1 regulate recombination activating gene expression in cancer cells. *PLoS One* 6, e20475.
- Correa, D., Hesse, E., Seriwatanachai, D., Kiviranta, R., Saito, H., Yamana, K., Neff, L., Atfi, A., Coillard, L., Sitara, D., Maeda, Y., Warming, S., Jenkins, N.A., Copeland, N.G., Horne, W.C., Lanske, B., Baron, R., 2010. Zfp521 is a target gene and key effector of parathyroid hormone-related peptide signaling in growth plate chondrocytes. *Dev. Cell* 19, 533–546.
- Day, T.F., Guo, X., Garrett-Beal, L., Yang, Y., 2005. Wnt/ β -catenin signaling in mesenchymal progenitors controls osteoblast and chondrocyte differentiation during vertebrate skeletogenesis. *Dev. Cell* 8, 739–750.
- Ducy, P., Desbois, C., Boyce, B., Piner, G., Story, B., Dunstan, C., Smith, E., Bonadio, J., Goldstein, S., Gundersen, C., Bradley, A., Karsenty, G., 1996. Increased bone formation in osteocalcin-deficient mice. *Nature* 382, 448–452.
- Ducy, P., Karsenty, G., 1995. Two distinct osteoblast-specific cis-acting elements control expression of a mouse osteocalcin gene. *Mol. Cell. Biol.* 15, 1858–1869.
- Ducy, P., Zhang, R., Geoffroy, V., Ridall, A.L., Karsenty, G., 1997. *Osfr/Cbfa1*: a transcriptional activator of osteoblast differentiation. *Cell* 89, 747–754.
- Duhen, T., Duhen, R., Lanzavecchia, A., Sallusto, F., Campbell, D.J., 2012. Functionally distinct subsets of human FOXP3+ Treg cells that phenotypically mirror effector Th cells. *Blood* 119, 4430–4440.
- Eijkelenboom, A., Burgering, B.M., 2013. FOXOs: signalling integrators for homeostasis maintenance. *Nat. Rev. Mol. Cell Biol.* 14, 83–97.
- Feng, X., Ippolito, G.C., Tian, L., Wiehagen, K., Oh, S., Sambandam, A., Willen, J., Bunte, R.M., Maika, S.D., Harriss, J.V., Caton, A.J., Bhandoola, A., Tucker, P.W., Hu, H., 2009. *Foxp1* is an essential transcriptional regulator for the generation of quiescent naive T cells during thymocyte development. *Blood* 115, 510–518.
- French, C.A., Groszer, M., Preece, C., Coupe, A.M., Rajewsky, K., Fisher, S.E., 2007. Generation of mice with a conditional *Foxp2* null allele. *Genesis* 45, 440–446.
- Funato, N., Chapman, S.L., McKee, M.D., Funato, H., Morris, J.A., Shelton, J.M., Richardson, J.A., Yanagisawa, H., 2009. *Hand2* controls osteoblast differentiation in the branchial arch by inhibiting DNA binding of *Runx2*. *Development* 136, 615–625.
- Gabut, M., Samavarchi-Tehrani, P., Wang, X., Slobodeniuc, V., O'Hanlon, D., Sung, H.K., Alvarez, M., Talukder, S., Pan, Q., Mazzoni, E.O., Nedelec, S., Wichterle, H., Woltjen, K., Hughes, T.R., Zandstra, P.W., Nagy, A., Wrana, J.L., Blencowe, B.J., 2011. An alternative splicing switch regulates embryonic stem cell pluripotency and reprogramming. *Cell* 147, 132–146.
- Guo, X., Day, T.F., Jiang, X., Garrett-Beal, L., Topol, L., Yang, Y., 2004. Wnt/ β -catenin signaling is sufficient and necessary for synovial joint formation. *Genes Dev.* 18, 2404–2417.
- Guo, X., Mak, K.K., Taketo, M.M., Yang, Y., 2009. The Wnt/ β -catenin pathway interacts differentially with PTHrP signaling to control chondrocyte hypertrophy and final maturation. *PLoS One* 4, e6067.
- Hartmann, C., 2009. Transcriptional networks controlling skeletal development. *Curr. Opin. Genet. Dev.* 19, 437–443.
- Hesse, E., Saito, H., Kiviranta, R., Correa, D., Yamana, K., Neff, L., Toben, D., Duda, G., Atfi, A., Geoffroy, V., Horne, W.C., Baron, R., 2010. Zfp521 controls bone mass by HDAC3-dependent attenuation of *Runx2* activity. *J. Cell Biol.* 191, 1271–1283.
- Hinoi, E., Bialek, P., Chen, Y.T., Rached, M.T., Groner, Y., Behringer, R.R., Ornitz, D.M., Karsenty, G., 2006. *Runx2* inhibits chondrocyte proliferation and hypertrophy through its expression in the perichondrium. *Genes Dev.* 20, 2937–2942.
- Hu, H., Wang, B., Borde, M., Nardone, J., Maika, S., Allred, L., Tucker, P.W., Rao, A., 2006. *Foxp1* is an essential transcriptional regulator of B cell development. *Nat. Immunol.* 7, 819–826.
- Javed, A., Chen, H., Ghori, F.Y., 2010. Genetic and transcriptional control of bone formation. *Oral Maxillofac. Surg. Clin. N. Am.* 22, 283–293.
- Karsenty, G., 2008. Transcriptional control of skeletogenesis. *Annu. Rev. Genomics Hum. Genet.* 9, 183–196.
- Karsenty, G., Wagner, E.F., 2002. Reaching a genetic and molecular understanding of skeletal development. *Dev. Cell* 2, 389–406.
- Katoh, M., Igarashi, M., Fukuda, H., Nakagama, H., 2013. Cancer genetics and genomics of human FOX family genes. *Cancer Lett.* 328, 198–206.
- Kobayashi, T., Kronenberg, H., 2005. Minireview: transcriptional regulation in development of bone. *Endocrinology* 146, 1012–1017.
- Kode, A., Mosialou, I., Silva, B.C., Rached, M.T., Zhou, B., Wang, J., Townes, T.M., Hen, R., DePinho, R.A., Guo, X.E., Kousteni, S., 2012. FOXO1 orchestrates the bone-suppressing function of gut-derived serotonin. *J. Clin. Investig.* 122, 3490–3503.
- Komori, T., Yagi, H., Nomura, S., Yamaguchi, A., Sasaki, K., Deguchi, K., Shimizu, Y., Bronson, R.T., Gao, Y.H., Inada, M., Sato, M., Okamoto, R., Kitamura, Y., Yoshiki, S., Kishimoto, T., 1997. Targeted disruption of *Cbfa1* results in a complete lack of bone formation owing to maturational arrest of osteoblasts. *Cell* 89, 755–764.
- Koon, H.B., Ippolito, G.C., Banham, A.H., Tucker, P.W., 2007. FOXP1: a potential therapeutic target in cancer. *Expert Opin. Ther. Targets* 11, 955–965.
- Korac, P., Peran, I., Skrtic, A., Ajdukovic, R., Kristo, D.R., Dominis, M., 2009. FOXP1 expression in monoclonal gammopathy of undetermined significance and multiple myeloma. *Pathol. Int.* 59, 354–358.
- Kronenberg, H.M., 2003. Developmental regulation of the growth plate. *Nature* 423, 332–336.
- Kume, T., 2011. The role of FoxC2 transcription factor in tumor angiogenesis. *J. Oncol.* 2012, 204593.

- Li, S., Wang, Y., Zhang, Y., Lu, M.M., DeMayo, F.J., Dekker, J.D., Tucker, P.W., Morrisey, E.E., 2012. Foxp1/4 control epithelial cell fate during lung development and regeneration through regulation of anterior gradient 2. *Development* 139, 2500–2509.
- Li, S., Weidenfeld, J., Morrisey, E.E., 2004. Transcriptional and DNA binding activity of the Foxp1/2/4 family is modulated by heterotypic and homotypic protein interactions. *Mol. Cell Biol.* 24, 809–822.
- Logan, M., Martin, J.F., Nagy, A., Lobe, C., Olson, E.N., Tabin, C.J., 2002. Expression of Cre Recombinase in the developing mouse limb bud driven by a Prxl enhancer. *Genesis* 33, 77–80.
- Long, F., 2012. Building strong bones: molecular regulation of the osteoblast lineage. *Nat. Rev. Mol. Cell Biol.* 13, 27–38.
- Long, F., Ornitz, D.M., 2013. Development of the endochondral skeleton. *Cold Spring Harb. Perspect. Biol.* 5, a008334.
- Lu, C., Wan, Y., Cao, J., Zhu, X., Yu, J., Zhou, R., Yao, Y., Zhang, L., Zhao, H., Li, H., Zhao, J., He, L., Ma, G., Yang, X., Yao, Z., Guo, X., 2013. Wnt-mediated reciprocal regulation between cartilage and bone development during endochondral ossification. *Bone* 53, 566–574.
- Lu, M.M., Li, S., Yang, H., Morrisey, E.E., 2002. Foxp4: a novel member of the Foxp subfamily of winged-helix genes co-expressed with Foxp1 and Foxp2 in pulmonary and gut tissues. *Mech. Dev.* 119 (Suppl. 1), S197–S202.
- Maes, C., Kobayashi, T., Selig, M.K., Torrekens, S., Roth, S.I., Mackem, S., Carmeliet, G., Kronenberg, H.M., 2010. Osteoblast precursors, but not mature osteoblasts, move into developing and fractured bones along with invading blood vessels. *Dev. Cell* 19, 329–344.
- Nakashima, K., Zhou, X., Kunkel, G., Zhang, Z., Deng, J.M., Behringer, R.R., de Crombrughe, B., 2002. The novel zinc finger-containing transcription factor osterix is required for osteoblast differentiation and bone formation. *Cell* 108, 17–29.
- Otto, F., Thornell, A.P., Crompton, T., Denzel, A., Gilmour, K.C., Rosewell, I.R., Stamp, G.W., Beddington, R.S., Mundlos, S., Olsen, B.R., Selby, P.B., Owen, M.J., 1997. Cbfa1, a candidate gene for cleidocranial dysplasia syndrome, is essential for osteoblast differentiation and bone development. *Cell* 89, 765–771.
- Raychaudhuri, P., Park, H.J., 2011. FoxM1: a master regulator of tumor metastasis. *Cancer Res.* 71, 4329–4333.
- Shimizu, E., Selvamurugan, N., Westendorf, J.J., Olson, E.N., Partridge, N.C., 2010. HDAC4 represses matrix metalloproteinase-13 transcription in osteoblastic cells, and parathyroid hormone controls this repression. *J. Biol. Chem.* 285, 9616–9626.
- Shu, W., Lu, M.M., Zhang, Y., Tucker, P.W., Zhou, D., Morrisey, E.E., 2007. Foxp2 and Foxp1 cooperatively regulate lung and esophagus development. *Development* 134, 1991–2000.
- Takahashi, K., Liu, F.C., Hirokawa, K., Takahashi, H., 2008. Expression of Foxp4 in the developing and adult rat forebrain. *J. Neurosci. Res.* 86, 3106–3116.
- Takarada, T., Hinoi, E., Nakazato, R., Ochi, H., Xu, C., Tsuchikane, A., Takeda, S., Karsenty, G., Abe, T., Kiyonari, H., Yoneda, Y., 2013. An analysis of skeletal development in osteoblast-specific and chondrocyte-specific runt-related transcription factor-2 (Runx2) knockout mice. *J. Bone Miner. Res.* 28, 2064–2069.
- Vega, R.B., Matsuda, K., Oh, J., Barbosa, A.C., Yang, X., Meadows, E., McAnally, J., Pomajzl, C., Shelton, J.M., Richardson, J.A., Karsenty, G., Olson, E.N., 2004. Histone deacetylase 4 controls chondrocyte hypertrophy during skeletogenesis. *Cell* 119, 555–566.
- Wang, B., Lin, D., Li, C., Tucker, P., 2003. Multiple domains define the expression and regulatory properties of Foxp1 forkhead transcriptional repressors. *J. Biol. Chem.* 278, 24259–24268.
- Wang, B., Weidenfeld, J., Lu, M.M., Maika, S., Kuziel, W.A., Morrisey, E.E., Tucker, P.W., 2004. Foxp1 regulates cardiac outflow tract, endocardial cushion morphogenesis and myocyte proliferation and maturation. *Development* 131, 4477–4487.
- Wang, H., Geng, J., Wen, X., Bi, E., Kossenkov, A.V., Wolf, A.L., Tas, J., Choi, Y.S., Takata, H., Day, T.J., Chang, L.Y., Sprout, S.L., Becker, E.K., Willen, J., Tian, L., Wang, X., Xiao, C., Jiang, P., Crotty, S., Victoria, G.D., Showe, L.C., Tucker, H.O., Erikson, J., Hu, H., 2014. The transcription factor Foxp1 is a critical negative regulator of the differentiation of follicular helper T cells. *Nat. Immunol.* 15, 667–675.
- Yang, X., Matsuda, K., Bialek, P., Jacquot, S., Masuoka, H.C., Schinke, T., Li, L., Brancorsini, S., Sassone-Corsi, P., Townes, T.M., Hanauer, A., Karsenty, G., 2004. ATF4 is a substrate of RSK2 and an essential regulator of osteoblast biology; implication for Coffin–Lowry Syndrome. *Cell* 117, 387–398.
- Yang, Y., Topol, L., Lee, H., Wu, J., 2003. Wnt5a and Wnt5b exhibit distinct activities in coordinating chondrocyte proliferation and differentiation. *Development* 130, 1003–1015.
- Yoshida, C.A., Yamamoto, H., Fujita, T., Furuichi, T., Ito, K., Inoue, K., Yamana, K., Zanma, A., Takada, K., Ito, Y., Komori, T., 2004. Runx2 and Runx3 are essential for chondrocyte maturation, and Runx2 regulates limb growth through induction of Indian hedgehog. *Genes Dev.* 18, 952–963.
- Zhang, Y., Li, S., Yuan, L., Tian, Y., Weidenfeld, J., Yang, J., Liu, F., Chokas, A.L., Morrisey, E.E., 2010. Foxp1 coordinates cardiomyocyte proliferation through both cell-autonomous and nonautonomous mechanisms. *Genes Dev.* 24, 1746–1757.